Journal of Chromatography, 359 (1986) 369–382
Elsevier Science Publishers B.V., Amsterdam — Printed in The Netherlands

CHROMSYMP. 895

HIGH-PERFORMANCE AFFINITY CHROMATOGRAPHY OF DIVALENT CONCANAVALIN A ON MATRICES OF VARIABLE LIGAND DENSITY

DAVID J. ANDERSON, JACQUELINE S. ANHALT and RODNEY R. WALTERS*
Department of Chemistry, Iowa State University, Ames, IA 50011 (U.S.A.)

SUMMARY

Divalent concanavalin A was chromatographed under isocratic conditions on matrices of variable ligand density, containing immobilized *p*-aminophenyl α-D-mannopyranoside or D-glucosamine. Methyl α-D-mannopyranoside was used as a competing inhibitor in the mobile phase. As the ligand density increased, retention was observed to change from a primarily monovalent interaction to a primarily divalent interaction. Several retention models were used to examine the data and to evaluate the extent of cooperative binding. Especially when possible heterogeneity in the distribution of ligand molecules was taken into account, it was found that several retention models fit the data reasonably well.

INTRODUCTION

While retention modeling of monovalent solute–ligand interactions in affinity chromatography is straightforward and has been extensively studied[1–6], only a few affinity chromatographic studies have been performed modeling retention of solutes interacting divalently with immobilized ligands[7–10]. Several models of retention for divalent solutes in affinity chromatography have been proposed. One model widely used in affinity chromatography is the "independent, equivalent-site" model in which the two adsorption steps have identical equilibrium constants and in which the binding of one site is unaffected by the binding of the other site[11–15]. A second model used in ion-exchange[16,17], reversed-phase[18], hydrophobic-interaction[19–22] and affinity[23,24] chromatography is the "high-cooperativity" model in which adsorption always occurs via two (or more) ligand molecules. Recently, a "general" divalent model has been proposed in which the adsorption process occurs in two steps but with no assumption as to the extent of cooperativity or independence of the two binding steps[9,10].

Although each of these models has been employed in affinity chromatographic studies, only one previous study has compared more than one model[10]. In the present work, high-performance affinity chromatographic studies of a divalent solute on matrices of variable ligand density were performed to critically examine how well each model fit the data.

0021-9673/86/$03.50

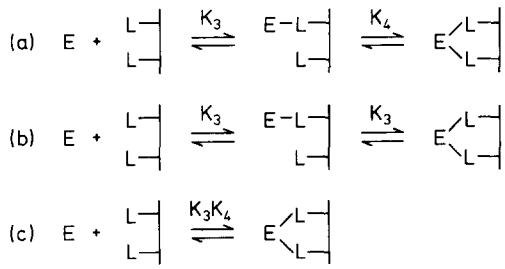

Fig. 1. Schematic diagram of three retention models: (a) general model, (b) independent, equivalent-site model, and (c) high-cooperativity model. In model (c), the quantity K_3K_4 represents a single equilibrium constant.

THEORY

The three major models for adsorption of divalent solute, E, onto a matrix containing immobilized ligands, L, are shown in Fig. 1. The equilibrium constant, K_3, is the monovalent binding constant, and K_4 is the binding constant of the second step. While K_3 is expressed in units of M^{-1}, K_4 is most correctly expressed in units of dm^2/mol, since surface concentrations are involved[9]. A monovalent inhibitor, I, is usually present in the mobile phase to control retention of E. The equilibrium constant for the binding of I to E is K_2[9]. An expression for the capacity factor (k') as a function of experimental variables has recently been derived for the general model[9]:

$$k' = \frac{K_3\{L\}A}{V_m} \cdot \frac{2(1 + K_2[I]) + K_4\{L\}}{(1 + K_2[I])^2} \tag{1}$$

where $\{L\}$ is the average ligand density (mol/dm^2), A is the surface area of the matrix, and V_m is the column void volume. In this model, the adsorption process is thought of as a monovalent binding step followed by possible binding of the second site on the solute to a second ligand molecule. Depending on the magnitude of K_4, the overall binding could range from purely monovalent ($K_4 = 0$) to primarily divalent ($K_4V_p/A \gg K_3$, where V_p is the column pore volume).

Expressions for the other models can be obtained easily, since they are limiting cases of the general model. Although free monovalent ligands in solution may bind to a divalent solute non-cooperatively (*i.e.*, binding of a second ligand molecule is not affected by binding of the first molecule), if the ligands are attached to a surface, the second binding step may be more strongly favored because of the close proximity of the solute to the second ligand molecule. Therefore, there may be cooperative binding of immobilized ligands to a multivalent solute even if the sites on the solute are all independent and equivalent. In the extreme case, which we will call the high-cooperativity model, all adsorption occurs divalently (*i.e.*, only EL_2 but no EL or ELI present):

$$k' = \frac{K_3K_4\{L\}^2A}{V_m(1 + K_2[I])^2} \tag{2}$$

TABLE I

LIMITING CASES OF THE GENERAL MODEL

Condition	*Explanation*
$K_4 = 0$	Monovalent binding of solute (second site empty or contains inhibitor), eqn. 4
$0 < K_4V_p/A < K_3$	Mixed monovalent and divalent (with negative cooperativity) binding
$K_4V_p/A = K_3$	Divalent, independent, equivalent binding of sites, with monovalent binding allowed, eqn. 3
$K_3 < K_4V_p/A$	Mixed monovalent and divalent (with positive cooperativity) binding
No EL or ELI	High-cooperativity model, no monovalent adsorption of solute, eqn. 2
No EL or ELI, $K_4V_p/A = K_3$	Divalent, equivalent-site model, in which no monovalent adsorption takes place

The quantity K_3K_4 in eqn. 2 really represents a single equilibrium constant, but for consistency we will express it as the product of the individual binding steps.

Some confusion can occur because the ligand always binds monovalently to the solute, while the solute can bind divalently to two ligands. In addition, when discussing cooperativity, one must think of the ligands binding cooperatively to the solute; but in chromatographic terms one thinks of the solute adsorbing on the ligands.

For the independent, equivalent-site model the expression is

$$k' = \frac{K_3\{L\}A}{V_m} \cdot \frac{2(1 + K_2[I]) + K_3\{L\}A/V_p}{(1 + K_2[I])^2} \tag{3}$$

The independent, equivalent-site model is basically a more limited form of the general model, in which the second ligand binding step has the same binding constant as the first step, *i.e.* $K_3 = K_4V_p/A$. (Note: the factor V_p/A is necessary to account for the different units of K_4 *vs.* K_3).

A possible fourth model is one in which only divalent binding takes place, but in which $K_3 = K_4V_p/A$. The equation would be similar to eqn. 2 but with K_4 replaced by K_3A/V_p. This will be called the divalent, equivalent-site model.

From eqn. 1, it is also seen that for purely monovalent binding,

$$k' = \frac{2K_3\{L\}A}{V_m(1 + K_2[I])} \tag{4}$$

The factor of two accounts for the two sites per solute molecule.

Table I summarizes the conditions under which the limiting cases of the general model apply.

A factor not taken into account in previous treatments is the possible heterogeneous distribution of ligand molecules. It is quite likely, especially at intermediate ligand densities, that some ligand molecules will be far enough from neighbouring ligands that divalent adsorption will not be possible. In that case, purely monovalent

interactions will occur in addition to the divalent interactions. To take this into account, one can assume that there is a fraction of the ligand molecules, f_L, occupying a fraction of the surface area, f_{SA}, with which the solute can interact divalently or monovalently, while with the remaining fraction of the sites $(1 - f_L)$ the solute can only interact monovalently. One can then derive heterogeneous versions of the above models. The heterogeneous, general model is described by

$$k' = \frac{K_3\{L\}A}{V_m} \cdot \frac{2(1 + K_2[I]) + f_L^2 K_4\{L\}/f_{SA}}{(1 + K_2[I])^2} \tag{5}$$

Monovalent interactions in the general model (eqn. 1) were due only to the position of the equilibrium between monovalently and divalently adsorbed forms of the solute. In the heterogeneous, general model, a fraction of the ligands is sterically unable to bind the solute divalently, while the remaining fraction can bind the solute monovalently and divalently as in the general model.

The heterogeneous, high-cooperativity model expression is

$$k' = \frac{K_3\{L\}A}{V_m} \cdot \frac{2(1 - f_L)(1 + K_2[I]) + f_L^2 K_4\{L\}/f_{SA}}{(1 + K_2[I])^2} \tag{6}$$

In this model, only monovalent adsorption occurs in regions of low ligand density and only divalent adsorption occurs in regions of high ligand density.

The equation for the heterogeneous, independent, equivalent-site model is

$$k' = \frac{K_3\{L\}A}{V_m} \cdot \frac{2(1 + K_2[I]) + f_L^2 K_3\{L\}A/V_p f_{SA}}{(1 + K_2[I])^2} \tag{7}$$

This is the same as the heterogeneous, general model except $K_3 = K_4 V_p/A$.

EXPERIMENTAL

Reagents

Concanavalin A (Con A, types IV and V), bovine serum albumin (BSA), D(+)-glucosamine hydrochloride, *p*-aminophenyl α-D-mannopyranoside (PAPM), and methyl α-D-mannopyranoside (MDM, grade III) were obtained from Sigma (St. Louis, MO, U.S.A.). The Con A was purified as described previously[9]. The 1,1'-carbonyldiimidazole (CDI) was obtained from Aldrich (Milwaukee, WI, U.S.A.). Hypersil WP-300, 5 μm, and LiChrospher SI 500, 10 μm, were from Alltech (Deerfield, IL, U.S.A.).

Procedure

The high and medium coverage PAPM columns and the glucosamine column were prepared as described earlier[9]. Note that the medium coverage column in this work was referred to as low coverage PAPM in the previous study. The low coverage PAPM column (this work) was prepared by a CDI activation method[25] with the following changes in a previously described procedure[9]. Diol-bonded Hypersil 300 was prepared according to a published procedure[26]. An amount of 1.9 g diol-bonded

Hypersil 300 was activated by the addition of 4.8 mg CDI. The amount of CDI added corresponded to 10% of the total diol content of the silica. The amounts used in the immobilization reaction were 0.6 g activated silica, 100 mg PAPM and 5 ml 0.1 *M* sodium phosphate buffer (pH 7). PAPM and glucosamine silicas were assayed as described previously[9].

Chromatographic apparatus and conditions were described previously[9]. The mobile phase consisted of MDM-containing acetate buffers (pH 5.0), prepared as described previously[9]. At this pH Con A existed as a dimer[27], containing two identical sugar binding sites[28]. Chromatography was performed with the column thermostated at 25.0°C. Con A samples (10 μl, 4 mg/ml), were injected. The samples were prepared in the appropriate MDM-containing buffer. Sample concentrations were found to be within linear elution conditions, as determined by concentration studies of Con A on the low coverage column[29]. Column parameters are summarized in Table II. The column void volume was determined by injection of water. The first moment of each peak was determined as the peak-center-at-half height. Capacity factors were calculated from first moments for Con A and water, and corrected for extra column time and a slight non-specific retention of Con A on diol columns (k' *ca.* 0.1 for LiChrospher SI 500 and negligible for Hypersil 300). A linear least squares analysis was used for fitting the experimental data to the monovalent model. A non-linear least squares analysis[30] was used for all other fits.

RESULTS AND DISCUSSION

Valency of Con A interaction with each column

Three PAPM matrices of different ligand densities, as well as a glucosamine matrix of high ligand density, were synthesized. All columns had the potential for divalent adsorption of Con A, except for the low coverage PAPM column, as deter-

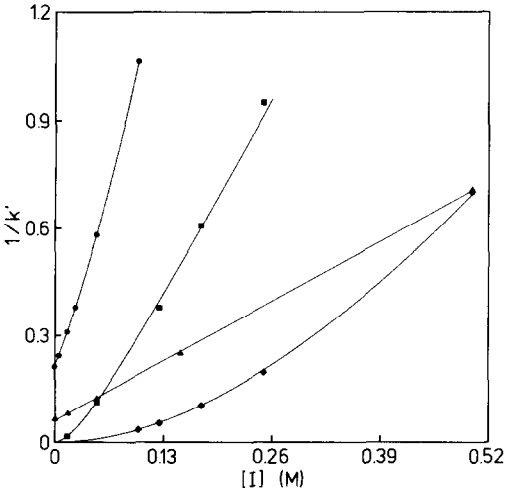

Fig. 2. Plots of $1/k'$ *vs.* the concentration of methyl α-D-mannopyranoside for the immobilized glucosamine column (●) and the immobilized PAPM columns of low (▲), medium (■), and high (◆) ligand densities. The inhibitor concentrations for the glucosamine and low coverage PAPM columns were actually 1/500 of those shown.

TABLE II

COLUMN PARAMETERS

Column	*Matrix*	*Dimensions (mm × mm)*	V_p* *(ml)*	V_m *(ml)*	A** (m^2)	$\{L\}$*** $(\mu mol/m^2)$	*Average distance between ligands (Å)*
Low coverage PAPM	5 μm Hypersil 300	50.0 × 4.1 I.D.	0.18	0.41	22	0.018	96
Medium coverage PAPM	10 μm LiChrospher SI 500	50.0 × 4.6 I.D.	0.38	0.67	15	0.28	24
High coverage PAPM	10 μm LiChrospher SI 500	45.0 × 4.6 I.D.	0.34	0.58	13	0.98	13
Glucosamine	10 μm LiChrospher SI 500	50.3 × 4.1 I.D.	0.29	0.50	12	0.73	15

* Determined by multiplying V_m by an experimentally determined ratio V_p/V_m for LiChrospher SI 500 and Hypersil 300 diol columns (ref. 27).
** Based on column volume, experimentally determined packing density and manufacturers' estimates of surface area.
*** Based on ligand assays and manufacturers' estimates of surface area.

mined from estimates of the average ligand spacing on the matrix. The average distance between ligands was calculated for each column, assuming an even distribution of immobilized ligand on the silica surface, and is given in Table II. Only the low coverage PAPM column had an average distance between ligands greater than 50 Å, which is the distance between sugar binding sites on the Con A dimer[31].

A preliminary assessment of the valency of Con A interaction with each affinity matrix was made by examination of $1/k'$ *vs.* [I] plots, which are given in Fig. 2. According to eqn. 4, a straight line would be expected for purely monovalent adsorption. This was observed only for the low coverage PAPM column, as anticipated from the estimates of the average ligand spacing on the silica surface. The other data sets showed curvature in the $1/k'$ *vs.* [I] plots, indicating multivalent interaction of the Con A with the matrix. The multivalent nature of this data is clearly illustrated by some simple calculations for the higher coverage PAPM columns using the monovalent values of K_2 and K_3 (obtained from the monovalent fit of the low coverage PAPM data) given in Table III. For the medium coverage PAPM column, the monovalent k' should be 0.20 at [I] = 0.05 M; the experimental value was 9.0. For the high coverage column, k' should be 0.14 at [I] = 0.25 M; the experimental value was 5.1.

Precision of the fit for various models for each column

Data for each column was fit to eqns. 1–4 to determine which model most precisely fit the experimental data. In order to quantitatively compare the fitting precision for each of the various models, a percent error of fit was calculated, as specified and tabulated in Table III. No assumption regarding values for the equilibrium constants (K_2, K_3 and K_4) was made in fitting the low coverage PAPM and glucosamine data sets. However, it was necessary to assume a value of K_2 for the medium and high coverage PAPM columns. This is because the experimental conditions were such that K_2 [I] $\gg$ 1, which resulted in the incorporation of the K_2 term within the other equilibrium constants (see eqns. 1–4). Based on previous work[29], a value for K_2 of $8.3 \cdot 10^3$ M^{-1} was used.

Comparison of the percent error of the fits for each model in Table III, as well as examination of the plots for each model given in Fig. 3, shows that the data sets for all four columns were most precisely fit by the general model (eqn. 1). This finding

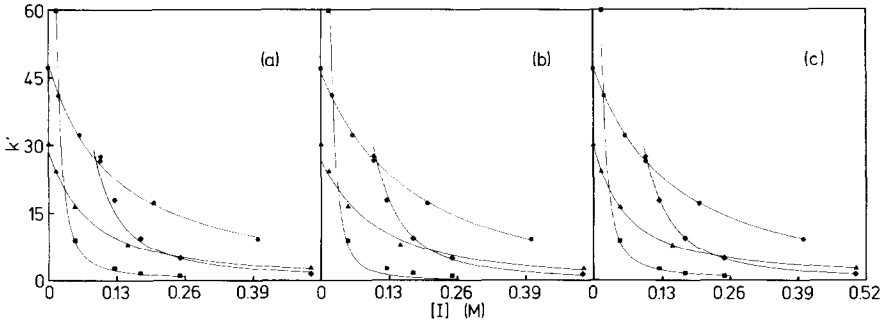

Fig. 3. Fits of the retention data to (a) the independent, equivalent-site model, (b) the high-cooperativity model, and (c) the general model. The symbols are the same as in Fig. 2. The capacity factors and inhibitor concentrations for the glucosamine column were actually 1/10 and 1/2000 of those shown, respectively, and 1/2 and 1/500, respectively, for the low coverage PAPM column.

TABLE III

EQUILIBRIUM CONSTANT DATA

	Low coverage PAPM	*Medium coverage PAPM**	*High coverage PAPM**	*Glucosamine*
Monovalent fit (eqn. 4)				
K_2 (M^{-1})	$1.0 \cdot 10^4$	–	–	$2.3 \cdot 10^4$
K_3 (M^{-1})	$8.5 \cdot 10^3$	$3.9 \cdot 10^5$	$3.8 \cdot 10^5$	$1.6 \cdot 10^2$
Error of fit (%)**	4.5	88.2	97.8	8.0
Independent sites (eqn. 3)				
K_2 (M^{-1})	$3.8 \cdot 10^3$	–	–	$1.1 \cdot 10^4$
K_3 (M^{-1})	$2.2 \cdot 10^3$	$1.2 \cdot 10^5$	$1.1 \cdot 10^5$	69
Error of fit (%)	4.7	14.4	19.9	3.0
High-cooperativity (eqn. 2)				
K_2 (M^{-1})	$2.3 \cdot 10^3$	–	–	$6.2 \cdot 10^3$
$K_3K_4V_p/A$ (M^{-2})	$6.6 \cdot 10^6$	$2.2 \cdot 10^{10}$	$2.4 \cdot 10^{10}$	$9.0 \cdot 10^3$
Error of fit (%)	12.8	57.8	10.3	1.9
General (eqn. 1)				
K_2 (M^{-1})	$5.6 \cdot 10^3$	–	–	$7.6 \cdot 10^3$
K_3 (M^{-1})	$4.3 \cdot 10^3$	$1.6 \cdot 10^5$	$3.9 \cdot 10^4$	24
K_4V_p/A (M^{-1})	$7.8 \cdot 10^2$	$7.0 \cdot 10^4$	$5.2 \cdot 10^5$	310
Error of fit (%)	0.6	3.4	1.5	0.3

* Using a value of $8.3 \cdot 10^3$ M^{-1} for K_2.

** Calculated from the experimental k' values (k'_{exp}) and the k' values from the fit (k'_{fit}) by the equation $100\{\Sigma[(k'_{exp} - k'_{fit})/k'_{exp}]^2/(n-1)\}^{1/2}$, where n is the number of experimental points.

was expected, however, because the high-cooperativity (eqn. 2), the independent, equivalent-site (eqn. 3) and the monovalent (eqn. 4) models are limiting cases of the general model and therefore can never exceed the general model in fitting precision. What needs to be determined, however, is whether retention can also be accurately depicted by any of the simpler models. This is particularly of interest for multivalent solutes, for which the independent, equivalent-site model has been extensively used to model affinity chromatographic retention[11–15].

Determination of the adequacy of these limiting-case models requires examination of the percent error of the fits (Table III), which in a simplistic way can be viewed as the average percent deviation of the experimental points from the fitted plot. An overview of all the columns showed the range of percent error for the general model to be lowest, varying from 0.3 to 3.4%. In contrast, the errors for the other models were several-fold larger.

Whether the limiting-case models gave fits with adequate precision (less than 5% error in the fit) depended on the column used. Good fits were obtained for the glucosamine data set for the high-cooperativity (1.9% error) and independent, equivalent-site (3.0% error) models. The fit of the glucosamine data to the monovalent model was moderately good. The 8% error for this fit, however, was nearly double the error for the same fit of the low coverage PAPM data set, reflecting a greater degree of divalent interaction for the glucosamine column.

The greatest deviation for the limiting-case models was noted for the higher coverage PAPM columns. The total failure of the monovalent model to predict retention for these columns is seen by the very high percent errors (90–100%) for these fits. High percent errors were also noted for the independent, equivalent-site (14–20% error) and high-cooperativity (10–58% error) models. The seriousness of this deviation was best exemplified by the medium coverage PAPM data, in which both the independent, equivalent-site and high-cooperativity models significantly overestimated k' for the lower MDM concentration (71.5 and 90.8, respectively, compared to an experimental value of 59.9). Thus, with fitting errors of 10% and greater for the limiting-case models, the appropriateness of these models for fitting the data from the two higher coverage PAPM columns was determined to be inadequate.

Comparison of the model fits for the low coverage PAPM data set indicated that there was a small amount of divalent adsorption of Con A occurring on this column. The good linear fit of eqn. 4 (0.9999 correlation coefficient) to the data, as well as the results of the ligand assays, which showed that the density of immobilized ligand molecules was low enough to exclude divalent interaction of Con A, supported the contention that the majority of Con A adsorption on this column was monovalent. The fitting error for the monovalent model, however, was 4.5%. Fitting the general model improved the percent error of the fit to 0.6%, by finding a small value of the $K_4\{L\}$ term. This finding suggests that, in addition to the monovalent adsorption, there was also a small fraction of higher density immobilized ligand molecules with which Con A could divalently interact. This mixed valency of interaction due to a heterogeneous distribution of immobilized ligand molecules is modeled by eqn. 5, which is of the same form as the general model, and will be discussed in more detail later.

Comparison of the percentage error of the fits (Table III) for the two multivalent limiting-case models (eqns. 2 and 3) shows that the independent, equivalent-

site model gave the most precise fit for the lower ligand density columns (low and medium coverage PAPM columns) while the high-cooperativity model gave the most precise fits for the higher ligand density columns (glucosamine and high coverage PAPM columns). This trend suggests an increase in cooperativity with an increase in surface density of affinity ligands.

The data presented so far supports the conclusion that choosing one of the limiting-case models for the determination of equilibrium constants may be too restrictive. While each of the models gave good fits in some cases, only the general model gave good fits in all of the cases. Although some of the goodness of fit was related to the number of fitted parameters, the data does suggest that equilibrium constants determined using the independent, equivalent-site model, or any of the other limiting-case models, may be in error.

Calculated equilibrium constants

Equilibrium constant values were calculated from the fits by using independently determined values for $\{L\}$, A, V_p and V_m (Table II) and are given in Table III. The equilibrium constant, K_4, which is written in terms of surface concentrations, was converted to a solution equilibrium constant by multiplying by the factor V_p/A. The solution equilibrium constant, K_4V_p/A, assumes that all affinity ligand molecules were evenly distributed within the volume V_p. The experimental values of K_2 for the binding of MDM to Con A in the mobile phase can be compared to a K_2 of $8.3 \cdot 10^3\ M^{-1}$ for the adsorption of MDM on immobilized Con A[29]. Experimental K_3 values for PAPM can be compared to K_3 ($2.4 \cdot 10^4\ M^{-1}$) for *p*-nitrophenyl α-D-mannopyranoside (PNPM) chromatographed on immobilized Con A [29] and K_3 ($8.7 \cdot 10^3\ M^{-1}$) for PNPM and Con A in free solution[32]. Experimental K_3 values for glucosamine can be roughly compared to the solution binding constant for N-acetyl-D-glucosamine of $1.4 \cdot 10^2\ M^{-1}$ determined at 5°C[33].

Equilibrium constants calculated for the glucosamine column varied according to the model used; however, K_2 and K_3 values were all reasonable in comparison with the values given above, with the exception of the K_2 value estimated from the monovalent fit, which was a factor of three too high. The general model yielded a value for K_2 ($7.6 \cdot 10^3\ M^{-1}$) that was closest to the expected value.

The discussion following will concentrate on the equilibrium constant results determined for the PAPM columns, as several discrepancies were noted in comparing the results for the different ligand coverage columns. All of the values for K_2 and K_3 obtained from the low coverage PAPM data were within a factor of five of the expected values. The monovalent and general models yielded estimates of K_2 closest to the expected value. The general model provided the best fit to the data and indicated weak divalent adsorption (K_4V_p/A *ca.* 1/5 of K_3). The use of the general model for this data set seemed reasonable, particularly when examined in the context of possible heterogeneity (see below).

The value for K_3 obtained for the low coverage PAPM column can be compared to the K_3 values obtained for the higher coverage PAPM columns. One would expect the value of K_3 to remain constant as the ligand density changed. However, none of the models showed this expected constancy in the K_3 term (Table III). Although a similar value for K_3 was calculated for both the medium and high coverage PAPM columns using the independent, equivalent-site model, the value was at least

one order of magnitude greater than the value calculated for the low coverage PAPM column. This increase in K_3 undermines the independence presumption of the model, which states that the binding strength of one site is unaffected by the binding of the other site. The general model also showed an increase in the value of K_3 from the low to the higher coverage PAPM columns. In addition, the value for K_3 varied widely for the three columns, showing no particular trend with surface concentration of immobilized ligand. At present, these inconsistencies cannot be explained, although several suggestions are offered later in this paper.

While in theory K_3 values should be constant for different immobilized ligand concentrations, it is not known how K_4 should vary with immobilized ligand concentration, much less what the value for K_4 should be. The extent of cooperativity will be reflected in the value of K_4V_p/A relative to K_3. K_4 will necessarily be zero due to steric considerations below a certain ligand density. One might imagine that K_4 would increase to a constant value above this critical density of ligand molecules. On the other hand, K_4 might continue to increase with ligand density as more ligand molecules became accessible to the second solute binding site.

No matter which model is chosen, the data suggested a significant degree of cooperative binding of the ligands to Con A. From the independent, equivalent-site fit, this was suggested by the higher values of K_3 determined for the higher coverage columns compared to the low coverage column. From the high-cooperativity model, this was suggested by the values of $K_3K_4V_p/A$ for the higher coverage columns, which were larger than the value of $(K_3)^2$ from the monovalent data. For the same reason, this suggests that the divalent, equivalent-site model was a poor model. Finally, from the general model, the value of K_4 was observed to increase with ligand density, as one would expect if K_4 itself were a function of ligand density. Note that the value of K_4V_p/A was smaller than K_3 for the low coverage column, but larger than K_3 for the high coverage column. This also suggested that the divalent adsorption process became more favorable as the ligand density increased.

Explanations for discrepancies found for the equilibrium constants

Several factors could explain the discrepancies found in the K_3 results. Accurate determinations of the equilibrium constants, K_3 and K_4, depended on the ability to determine $\{L\}$, V_m, V_p and A with minimum error. For the present study, determination of $\{L\}$ presented the greatest difficulty, since the desired immobilized ligand concentration (which will be referred to as the functional ligand concentration) was that which was active and accessible to the Con A molecule. To determine the functional ligand concentration required a breakthrough analysis. This was not feasible for the present system for several reasons. First, the concentration of Con A required to saturate most of the ligand molecules was too high for practical considerations. Second, saturation of the higher ligand density columns would not be a true determination of the amount of accessible ligand molecules, as an unknown number of immobilized ligand molecules would be covered, but not bound to, the Con A molecules. The best estimate for the functional ligand concentration was the determination of the total ligand concentration by chemical analysis, which was the procedure used in this work. Differences in the percent of the total ligand content that were functional for the three PAPM columns could explain the variability in K_3. This may be particularly true in comparing the low coverage PAPM column to the higher coverage PAPM columns, in which different silica matrices were used.

Retention by other mechanisms, such as hydrophobic interactions, could also present a problem. This is of particular concern for the Con A system, which in addition to its sugar binding sites, has two hydrophobic binding sites for each dimer molecule[31]. This effect would be multiplicative in the same way that the retention of Con A was multiplicative through the K_3K_4 term, as seen in eqn. 1, but might show a different dependence on the concentration of the hydrophilic inhibitor MDM. This could explain the increase of K_3 found for the higher coverage PAPM columns, in which simultaneous mixed retention mechanisms could occur, over the low coverage PAPM column, in which simultaneous mixed retention mechanisms were precluded by the low density of the immobilized ligand molecules.

An additional cause for high K_3 values could be the presence of tetravalent Con A. Although the pH of the mobile phase was chosen such that Con A was present predominantly as the dimer, the presence of small amounts of tetravalent Con A could increase retention and alter the shape of the k' *vs.* [I] plots. This would affect the values of the equilibrium constants calculated.

Heterogeneity

One of the most likely models would seem to be one in which an uneven distribution of ligands results in a mixture of monovalent and of divalent interactions, some of which could only be monovalent while others could be monovalent or divalent. This would be especially likely on low to medium coverage columns. The general, high-cooperativity, and independent, equivalent-site models incorporating this effect of heterogeneity of interaction are given as eqns. 5–7, respectively. These equations are seen to be identical in form to the general model given in eqn. 1, which fit the data excellently (Fig. 3c). Thus, one can reinterpret the fits to the general model (Table III) in terms of the various heterogeneous models.

Since there are two new parameters (f_L and f_{SA}) in the heterogeneous equations whose values would be difficult to determine experimentally, and since all three heterogeneous models are of the same form as the general model (a quadratic equation), one cannot rule out any of the models based on fits to the chromatographic data. However, in some instances some of the equilibrium constants could still be determined. Examination of eqns. 5 and 7 indicate that it should still be possible to determine K_2 and K_3 in the heterogeneous versions of the general and independent, equivalent-site model, while K_2 could still be determined in the case of the heterogeneous, high-cooperativity model.

Examination of the heterogeneous equations also indicated that heterogeneity could not be the cause of the unexpected increase in K_3 values noted for the higher coverage PAPM columns.

For all of the heterogeneous models, one could interpret changes in the value K_4V_p/A from the data in Table III to be due either to changes in the *strength* of divalent interaction (K_4) or due to changes in the *extent* of divalent interaction (f_L and f_{SA}). This latter interpretation is particularly attractive for the low coverage PAPM column, since it could explain why some divalent interactions appeared to take place even though the average ligand density was lower than what was necessary. This could also explain why K_4 appeared to increase with ligand density (*i.e.*, $f_L^2K_4/f_{SA}$ was actually being determined).

CONCLUSIONS

The equilibrium constants determined for the competing sugar from the low coverage PAPM and glucosamine studies were in good agreement with literature values. However, K_3 values for the medium and high coverage PAPM columns were larger than expected from the monovalent data. This discrepancy was not accounted for by any of the models.

Hogg and Winzor[10] have reported closer fits of affinity chromatographic data using an independent, equivalent-site model as compared to the high-cooperativity model. This was not found to be true for all of the data in the present work. Only the general and heterogeneous models gave reasonably good fits to the data over a wide range of ligand density.

Values calculated for the equilibrium constants varied with the retention model used to fit the data. Thus, without additional experimental information to elucidate the exact mechanism of retention, it was not possible to obtain reliable equilibrium constants for divalent solutes.

ACKNOWLEDGEMENT

This work was supported by the National Science Foundation under Grant CHE-8305057.

REFERENCES

1 P. Andrews, B. Kitchen and D. Winzor, *Biochem. J.*, 135 (1973) 897.
2 B. M. Dunn and I. M. Chaiken, *Proc. Natl. Acad. Sci. U.S.A.*, 71 (1974) 2382.
3 J. Turkova, *Affinity Chromatography*, Elsevier, Amsterdam, 1978, p. 35.
4 I. M. Chaiken, *Anal. Biochem.*, 97 (1979) 1.
5 K. Nilsson and P.-O. Larsson, *Anal. Biochem.*, 134 (1983) 60.
6 B. M. Dunn, *Appl. Biochem. Biotechnol.*, 9 (1984) 261.
7 D. Eilat and I. M. Chaiken, *Biochemistry*, 18 (1979) 790.
8 J. K. Inman, in I. M. Chaiken, M. Wilchek and I. Parikh (Editors), *Affinity Chromatography and Biological Recognition*, Academic Press, New York, 1983, p. 153.
9 D. J. Anderson and R. R. Walters, *J. Chromatogr.*, 331 (1985) 1.
10 P. J. Hogg and D. J. Winzor, *Arch. Biochem. Biophys.*, 240 (1985) 70.
11 I. M. Chaiken, D. Eilat and W. M. McCormick, *Biochemistry*, 18 (1979) 794.
12 L. W. Nichol, L. D. Ward and D. J. Winzor, *Biochemistry*, 20 (1981) 4856.
13 D. J. Winzor, L. D. Ward and L. W. Nichol, *J. Theor. Biol.*, 98 (1982) 171.
14 P. J. Hogg and D. J. Winzor, *Arch. Biochem. Biophys.*, 234 (1984) 55.
15 D. J. Winzor and R. J. Yon, *Biochem. J.*, 217 (1984) 867.
16 W. Kopaciewicz, M. A. Rounds, J. Fausnaugh and F. E. Regnier, *J. Chromatogr.*, 266 (1983) 3.
17 M. A. Rounds and F. E. Regnier, *J. Chromatogr.*, 283 (1984) 37.
18 X. Geng and F. E. Regnier, *J. Chromatogr.*, 296 (1984) 15.
19 H. P. Jennissen and L. M. G. Heilmeyer, Jr., *Biochemistry*, 14 (1975) 754.
20 H. P. Jennissen, *Biochemistry*, 15 (1976) 5683.
21 H. P. Jennissen, *J. Chromatogr.*, 159 (1978) 71.
22 H. P. Jennissen, *J. Chromatogr.*, 215 (1981) 73.
23 P. Kyprianou and R. J. Yon, *Biochem. J.*, 207 (1982) 549.
24 R. J. Yon and P. Kyprianou, in I. M. Chaiken, M. Wilchek, and I. Parikh (Editors), *Affinity Chromatography and Biological Recognition*, Academic Press, New York, 1983, p. 143.
25 G. S. Bethell, J. S. Ayers, M. T. W. Hearn and W. S. Hancock, *J. Chromatogr.*, 219 (1981) 353.
26 R. R. Walters, in P. D. G. Dean, W. S. Johnson and F. A. Middle (Editors), *Affinity Chromatography: A Practical Approach*, IRL Press, Oxford, 1985, p. 25.

27 M. Huet, *Eur. J. Biochem.*, 59 (1975) 627.
28 F. G. Loontiens, R. M. Clegg and T. M. Jovin, *Biochemistry*, 16 (1977) 159.
29 D. J. Anderson and R. R. Walters, *J. Chromatogr.*, 376 (1986) 69.
30 S. D. Christian and E. E. Tucker, *Am. Lab.*, 14 (9) (1982) 31.
31 K. D. Hardman and C. F. Ainsworth, *Biochemistry*, 15 (1976) 1120.
32 S. D. Lewis, J. A. Shafer and I. J. Goldstein, *Biochem. Biophys.*, 172 (1976) 689.
33 Y. Oda, K. Kasai and S. Ishii, *J. Biochem.*, 89 (1981) 285.